

Surface Characteristics and Adhesion Behavior of *Escherichia coli* O157:H7: Role of Extracellular Macromolecules

Hyunjung N. Kim,[†] Yongsuk Hong,[†] Ilkeun Lee,[‡] Scott A. Bradford,[§] and Sharon L. Walker^{*,†}

Department of Chemical and Environmental Engineering, and Department of Chemistry, University of California, Riverside, California 92521, and USDA, ARS, US Salinity Laboratory, Riverside, California 92507

Received May 5, 2009; Revised Manuscript Received June 30, 2009

Experiments were conducted using enterohemorrhagic *Escherichia coli* O157:H7 cells to investigate the influence of extracellular macromolecules on cell surface properties and adhesion behavior to quartz sand. Partial removal of the extracellular macromolecules on cells by a proteolytic enzyme (proteinase K) was confirmed using Fourier transform infrared spectroscopy analyses. The proteinase K treated cells exhibited more negative electrophoretic mobility (EPM) at an ionic strength (IS) ≤ 1 mM, a slightly lower isoelectric point, and were less hydrophobic as compared to the untreated cells. Potentiometric titration results indicated that the total site concentration (i.e., the total amount of exposed functional groups per cell) on the treated cells was approximately 22% smaller than the untreated cells, while the dissociation constants were almost identical. Analysis of the EPM data using soft particle theory showed that the removal of extracellular macromolecules resulted in polymeric layers outside the cell surface that were less electrophoretically soft. The more negative mobility for the treated cells was likely due to the combined effects of a change in the distribution of functional groups and an increase in the charges per unit volume after enzyme treatment and not just removal of extracellular macromolecules. The proteolytic digestion of extracellular macromolecules led to a significant difference in the cell adhesion to quartz sand. The adhesion behavior for treated cells was consistent with DLVO theory and increased with IS due to less negativity in the EPM. In contrast, the adhesion behavior of untreated cells was much more complex and exhibited a maximum at IS = 1 mM. The treated cells exhibited less adhesion than the untreated cells when the IS ≤ 1 mM due to their more negative EPM. However, when the IS ≥ 10 mM, a sudden decrease in the removal efficiency was observed only for the untreated cells even though EPM values were similar for both treated and untreated cells. This result suggested that an additional non-DLVO type interaction, electrosteric repulsion, occurred at higher IS (≥ 10 mM in this study) for the untreated cells due to the presence of extracellular macromolecules that hindered cell adhesion to the quartz surface. This finding provides important insight into the role of macromolecule-induced *E. coli* O157:H7 interactions in aquatic environments.

Introduction

Enterohemorrhagic *Escherichia coli* O157:H7 is a Gram-negative pathogenic bacterium that was first recognized as a cause of human disease in 1982.^{1,2} *E. coli* O157:H7 is known to produce verotoxins or Shiga-like toxins, which make the bacterium highly virulent.^{3,4} The major symptoms caused by *E. coli* O157:H7 are reported as bloody and nonbloody diarrhea, hemorrhagic colitis, and hemolytic uremic syndrome, which can result in acute renal failure in children.^{3,5,6} In general, outbreaks by *E. coli* O157:H7 have been associated with both water^{7–9} and especially food.⁹ The waterborne outbreaks by *E. coli* O157:H7 are primarily associated with surface water.^{10,11} However, recent studies indicate that contaminated groundwater is also associated with *E. coli* O157:H7 outbreaks.^{4,12} Surface and groundwater outbreaks of *E. coli* O157:H7 and other enteric pathogens have been reported to be associated with high intensity rainfall events.^{13,14} Hence, an understanding of the fate of *E. coli* O157:H7 in subsurface and groundwater environments is needed to help protect and assess the risk of contamination of drinking water supplies.

E. coli O157:H7 cells possess a variety of external and surface bound macromolecules such as flagella, pili, fimbriae, proteins, extracellular polymeric substances (EPS), and lipopolysaccharides (LPS).^{15,16} These extracellular macromolecules are very complex and heterogeneous. For example, EPS is a rich polymeric matrix that includes polysaccharides, proteins, glycoproteins, nucleic acids, phospholipids, and humic acids.^{17,18} Interaction mechanisms between cells and solid surfaces are typically assumed to depend on the physicochemical properties of cell surfaces^{19–22} that can be approximated by the balance of electrostatic and van der Waals interactions (i.e., classic DLVO-type forces)^{23,24} and on the hydrophobic properties^{25,26} of the surfaces. Unlike ideal colloids, however, it has been often reported that real interaction phenomena deviate from predictions due to various extracellular macromolecules. One example is the prediction of cell surface potentials based on a hard sphere model^{27,28} often deviates from the real surface potential of the microorganisms.^{29–31} Another is the observed magnitude of attractive or repulsive forces between microbes and surfaces at short and long separation distances.^{32–39} In addition, the type and extent of the interaction may depend on the amount, composition, and configuration of the bound surface macromolecules.^{35–37,39} These observations clearly suggest that the influence of chemical and structural heterogeneities on physi-

* Corresponding author. Phone (951) 827-6094; Fax (951) 827-5696; E-mail swalker@engr.ucr.edu.

[†] Department of Chemical and Environmental Engineering.

[‡] Department of Chemistry.

[§] USDA.

Table 1. Viability, Size, and Aspect Ratio of Proteinase K Treated and Untreated *E. coli* O157:H7 Cells as a Function of IS at Room Temperature (22–25 °C)^a

IS (mM)	untreated <i>E. coli</i> O157:H7				proteinase K treated <i>E. coli</i> O157:H7			
	live (%) ^b	culturability ^c	radius (μm) ^d	aspect ratio ^e	live (%) ^b	culturability ^c	radius (μm) ^d	aspect ratio ^e
0.01	96.4 ± 0.8	ND	0.34 ± 0.04	3.5 ± 1.5	96.9 ± 1.2	ND	0.34 ± 0.06	3.1 ± 1.7
0.1	98.1 ± 0.7	ND	0.35 ± 0.05	3.3 ± 1.7	97.0 ± 1.1	ND	0.33 ± 0.06	3.3 ± 1.4
1	92.8 ± 2.1	ND	0.39 ± 0.06	3.7 ± 2.2	90.8 ± 1.8	ND	0.35 ± 0.05	3.3 ± 2.0
10	92.6 ± 1.4	82%	0.34 ± 0.05	2.9 ± 1.9	91.8 ± 1.5	77%	0.34 ± 0.07	3.0 ± 1.7
100	95.9 ± 2.4	ND	0.37 ± 0.04	2.9 ± 1.6	93.2 ± 2.0	ND	0.36 ± 0.06	2.7 ± 1.8

^a All experiments were conducted at unadjusted pH (5.6–5.8). ^b Percent of cell population determined to be viable based on the Live/Dead BacLight kit. ^c Percent of viable cell numbers determined by plate count. ^d Value for equivalent spherical radius calculated from experimentally measured length and width of individual cells. ^e Ratio of cell length and width measured. The data for untreated cells conducted at 1, 10, and 100 mM were obtained from ref 38. ND stands for “not determined.”

cochemical cell surface properties should be understood to gain further insight into mechanisms controlling cell–surface interactions.

Ohshima^{40–43} developed an improved electrokinetic model (i.e., soft particle theory) that allows one to predict the surface potential of microbes by considering the presence of ion-penetrable polymeric layers. The theory has been widely used to predict the surface potential of microbes and to evaluate the degree of electrophoretic softness of polymeric layers.^{31,44–46} In addition, several studies have recently attempted to characterize the chemistry of cell membrane or polymeric layers by combining macroscopic (e.g., zeta potential, surface hydrophobicity, potentiometric titration) and molecular (e.g., scanning electron microscopy, transmission electron microscopy, Fourier transform infrared spectroscopy, X-ray photoelectron spectroscopy) techniques.^{47–49} However, it is still not straightforward to quantify and generalize macromolecule-related variations in cell surface properties due to the complexity of the cell surface and the sensitivity of macromolecules to the cell type (e.g., species, serotypes, or strains)^{19,35,50} and environmental conditions (e.g., growth stage, temperature, and solution chemistry).^{15,19,20,51}

Our recent studies^{32,38,52} showed that the deposition behavior of *E. coli* O157:H7 in porous media could not be explained by traditional approaches (i.e., classic DLVO theory^{23,24} and filtration theory⁵³) and indicated that the presence of macromolecules on the cell surface likely influenced their surface characteristics and adhesion behavior. To date, however, little systematic work has been done to investigate these issues using *E. coli* O157:H7 and additional research is warranted. Therefore, this study was designed to systematically investigate the role of extracellular macromolecules on the surface properties and adhesion behavior. To achieve this purpose, a proteolytic enzyme (proteinase K) was employed to partially remove extracellular macromolecules associated with the outer surface of *E. coli* O157:H7 cells. Surface properties of untreated and proteinase K treated *E. coli* O157:H7 cells were extensively characterized and compared via electrophoretic mobility (EPM), hydrophobicity, potentiometric titration, and soft particle theory.^{40–43} In addition, adhesion tests were carried out for untreated and proteinase K treated cells across the ionic strength (IS) range of 0.01 to 100 mM in a batch system with quartz sand.

Materials and Methods

Bacterial Growth and Preparation. *E. coli* O157:H7/pGFP strain 72^{52,54} was used as a model bacterium in this study. The cells were precultured overnight in Tryptic Soy Broth (TSB, Becton Dickinson, Sparks, MD) at 37 °C and 200 rpm in the presence of 0.1 g/L ampicillin

(Sigma Aldrich, St. Louis, MO). The precultured media were transferred onto Tryptic Soy Agar (TSA, Becton Dickinson) in Petri dishes with 0.1 g/L ampicillin, and the cells were grown for 18 h at 37 °C to reach stationary phase. Bacteria were harvested and suspended in sterile deionized (DI) water and then collected by centrifugation (Fisher accuSpin 3R Centrifuge, Fisher Scientific, Pittsburgh, PA) at 3700 g for 15 min. The harvested cells were washed twice using 10 mM KCl (Fisher Scientific, Fair Lawn, NJ) to remove any residual growth media. Finally, the cells were resuspended in the select solutions for subsequent cell surface characterization and adhesion experiments described below.

The cell number was determined using a counting chamber (Buerker-Tuerk chamber, Marienfeld Laboratory Glassware, Germany) with a digital/video microscope (Micromaster* I and II, Fisher Scientific). Bacterial cell size and shape were determined from images taken with an inverted microscope (IX70, Olympus, Japan) in phase contrast mode. The lengths and the widths of the cells ($n \geq 50$) were measured using an image processing program (SimplePCI, Precision Instruments, Inc., Minneapolis, MN), and the corresponding equivalent radii and aspect ratios of the cells were calculated.

Enzyme Treatment for Digestion of Extracellular Macromolecules. To investigate the role of bacterial extracellular macromolecules on cell surface properties and adhesion behavior, a proteolytic enzyme (proteinase K, Sigma-Aldrich) was used to cleave extracellular macromolecules from bacteria. Proteinase K is known to have specificity to cleave peptide bonds at the carboxylic side of aliphatic, aromatic, or hydrophobic amino acids.⁵⁵ The structure of molecules cleaved by proteinase K can vary with the type of side chain (R group), which is attached to the first (α) carbon. A detailed description of the protocol that was employed is available in the literature.³⁴ Briefly, the concentration of bacterial suspension was adjusted to 5×10^8 cells/mL in a background solution (denoted as Trizma-buffer below) of 5 mM EDTA (Sigma-Aldrich), 0.01 g/L sodium dodecyl sulfate (Sigma-Aldrich), and 10 mM Tris-HCl (Sigma-Aldrich). The digestion process was then conducted at pH 8.0 with a final concentration of 0.1 mg/mL proteinase K in the bacterial suspension. This suspension was incubated at 37 °C and 260 rpm for 3 h in an incubation chamber (Model 4639, Barnstead/Labline, Melrose Park, IL). The proteinase K treated cells were washed twice by centrifugation at 13400 g for 2 min to remove the cleaved polymers, followed by one more rinsing with DI water at 3700 g for 10 min. Viability tests were performed to examine the integrity of the cell walls after exposure to proteinase K with two methods: (i) Live/Dead BacLight (L-7012, Molecular Probes, Eugene, OR) method⁵⁶ with an inverted fluorescent microscope and a red/green fluorescence filter set (Chroma Technology Corp., Brattleboro, VT); and (ii) plate count method.⁵⁷ Results in Table 1 showed that cells before and after enzyme treatment exhibited similar viability when using both methods; that is, >90% with the Live/Dead BacLight method and 77–82% from plate counts. The statistical test for plate count revealed that the difference (ca. 5%) was not statistically significant ($P > 0.05$). Viability test results suggested that proteolytic digestion had a minimal impact on cell wall damage.

Bacterial Cell Surface Characterization. EPM of untreated and proteinase K treated bacteria was measured at 25 °C as a function of IS using a ZetaPALS analyzer (Brookhaven Instruments Corporation, Holtsville, NY). The IS of the solution was controlled using KCl over a range of 0.01 to 100 mM and the pH of the solution was unadjusted (5.6–5.8). The concentration of bacterial suspension for the mobility was spectroscopically adjusted to an absorbance value between 0.25 and 0.3 at 546 nm (BioSpec-mini, Shimadzu Corp., Kyoto, Japan). A minimum of three different samples were measured for each condition and average values of 10 runs were obtained for one sample. Additionally, to find the isoelectric point (IEP) of untreated and treated cells, the EPM was also measured as a function of pH.

The hydrophobicity of the *E. coli* O157:H7 cells was measured using the microbial adhesion to hydrocarbons (MATH) test.⁵⁸ Measurements were carried out over the IS range of 1–100 mM at ambient pH (5.6–5.8) for both untreated and enzyme-treated cells. In brief, 1 mL of *n*-dodecane (laboratory grade, Fisher Scientific) was added to 4 mL of a cell suspension, which was then mixed for 2 min with a vortex. The suspension was then allowed to separate for 15 min at room temperature. The percentage of bacteria partitioned to the hydrocarbon phase was calculated after the optical density of the suspension in the water phase was measured at 546 nm (BioSpec-mini, Shimadzu Corp.). All experiments were conducted at least in triplicate.

Potentiometric titration was conducted to characterize the acid–base properties of the untreated and proteinase K treated bacterial cell surface. The background solution for the titration (i.e., 100 mM KCl) was thoroughly purged of CO₂ using N₂ gas (Puritan Medical Products, Inc., Overland Park, KS) for at least 1 h prior to the experiments. The washed bacteria were resuspended in 50 mL of 100 mM KCl solution at a final concentration of approximately 2.0 × 10⁹ cells/mL. The bacterial suspension was placed in a sealed titration vessel and purged with N₂ gas until the system maintained a constant pH reading for a period of at least 10 min. The pH of this suspension was then lowered to pH 3.0 with 0.1 N HCl. Titrations were subsequently carried out with 0.1 N NaOH titrant over the pH range of 3.0–10.5 using a 798 Titrino automatic titrator (Metrohm Ltd., Switzerland). The titrations were conducted at room temperature in the presence of N₂ gas purging and continuous stirring. The titrator was programmed with a monotonic equivalence point titration (MET) mode, which adds the same volume of titrant at each step. The drift criterion for the MET mode was a change in the electric potential of the pH electrode of less than 1.0 mV over 15 s. All titration experiments were conducted in triplicate. The dissociation constants (p*K*_a) and their corresponding site concentration (*C*_i) of functional group outside and on the bacterial cell surface were determined by the chemical speciation software FITEQL 4.0.^{59–61} Back titration with 0.1 N HCl was also conducted immediately after the forward titration to verify the reversibility of titration. The results (Figure S1 in Supporting Information) show that titrations are fully reversible, indicating that titrations with pH ranges in this study do not cause changes in cell wall structures during the titrations.⁶²

Fourier Transform Infrared Spectroscopy. Fourier transform infrared (FT-IR) spectroscopy has been used to characterize bacterial cell wall chemistry and to identify functional groups of macromolecules on the cell surface.^{47,63,64} In this study, FT-IR spectroscopy was employed to confirm the effectiveness of enzyme treatment and to investigate the type of macromolecules removed by proteinase K treatment. All of the IR spectra were obtained using a commercial ZnSe (2 mm diameter, spectral range: 20000–650 cm⁻¹) attenuated total reflection (ATR) accessory (Pike Technologies, Madison, WI) in a FT-IR spectrometer (Bruker Tensor 27, Billerica, MA) equipped with a deuterated-triglycine-sulfate (DTGS, spectral range: 10000–370 cm⁻¹) detector (Bruker Optics, Billerica, MA). The ATR system has a limited detection depth of several micrometers because the evanescent field decays exponentially in the rare medium.⁶⁵ This allows us to get a constant thickness of IR samples, so that only

0.2 mL of sample was dropped for the measurements to make an approximately 2 mm high small dome on the ZnSe element.

The measurements were carried out using supernatants obtained during centrifugation of the cell suspension before and after proteinase K treatment. Specifically, a little amount (1 mL) of sample was taken from the cell suspension before and after enzyme treatment. After centrifugation at 13400 *g* and 4 °C for 2 min, supernatant samples were investigated. A Trizma buffer solution including proteinase K was used as the background spectrum. A spectral resolution of 4 cm⁻¹ was chosen, and 10 scans were averaged per spectrum between 5000 and 400 cm⁻¹ in the IR software package OPUS 3.1. Each sample was tested 3–5 times to check reproducibility. Baselines were not corrected.

Cell Adhesion Test. The relative role of extracellular macromolecules on cell adhesion to quartz sand was examined using a batch adhesion experiment with untreated and proteinase K treated cells. The experiments were conducted by placing 10 g of quartz sand and 10 mL of cell suspension (concentration = ~5 × 10⁸ cells/mL) into a 20 mL scintillation tube with the temperature kept at approximately 25 °C. Ultrapure (99.99% SiO₂) quartz sand (Iota quartz, Unimin Corp., NC) was used for these tests. The average sand diameter (*d*₅₀) was approximately 275 μm and the shape of the sand was irregular.⁶⁶ The quartz sand was thoroughly cleaned using 12 N HCl (Fisher Scientific) and baked at 800 °C for at least 8 h to remove any organic impurities from the sand.²² Five different solution IS were considered in this study (0.01, 0.1, 1, 10, and 100 mM). The suspension and sand were allowed to equilibrate for 3 h by gently rotating the tubes end over end (8 rpm) on a tube shaker (Labquake, Branstead/Thermolyne,ubuque, IW). The initial and final concentrations of cells in the suspension were determined using a Turner Quantech Fluorometer, which has a fluorescent filter set with excitation and emission wavelengths of 490 and 515 nm to match the fluorescence of the *E. coli* O157:H7/pGFP strain. A new calibration curve was made for each experiment. The coefficient of linear regression value was always close to unity (data not shown). All experiments were performed at least in duplicate. A control experiment with sand and bacteria-free electrolyte solution was performed to quantify the background concentration originating from the sand. Similarly, a control experiment was also conducted using only cell suspension to quantify the cell loss to the glass tube.

Statistical Analysis. In tables and figures, mean data are presented along with error bars associated with one standard deviation. Statistical differences between mean values were analyzed using a student *t* test. When *P* < 0.05, the differences are considered to be statistically significant.

Soft Particle Theory. As mentioned briefly in the introduction, soft particle theory has been developed to interpret the EPM behavior of polyelectrolyte-coated particles^{40–43} and has been applied to bacteria to predict their surface potential.^{31,44–46} The theory allows one to determine two parameters: electrophoretic softness (λ^{-1}) and volumetric fixed charge density (ρ_{fix}). The parameter λ characterizes the resistance applied to the liquid flow in the cell surface region, and the value of λ^{-1} represents the characteristic distance from the slipping plane to the outermost part of the polymeric layer. The value of λ^{-1} is therefore related to the degree of softness of the polymeric layer. The second parameter, ρ_{fix} , represents the density of the fixed charges (charges per unit volume) originating from the ionogenic groups in the polyelectrolyte layer. The two parameters can be determined from measured EPM (denoted by μ) as a function of IS using the following equation^{40–43}

$$\mu = \frac{\epsilon_r \epsilon_0 (\psi_0 / \kappa_m) + (\psi_{\text{DON}} / \lambda)}{\eta (1 / \kappa_m) + (1 / \lambda)} + \frac{\rho_{\text{fix}}}{\eta \lambda^2} \quad (1)$$

where ϵ_0 is the dielectric permittivity in vacuum, ϵ_r is the relative dielectric permittivity in water, η is the dynamic viscosity of water, ψ_0 is the outer surface potential, ψ_{DON} is the Donnan potential in the polyelectrolyte layer, and κ_m is the Debye–Hückel parameter of the

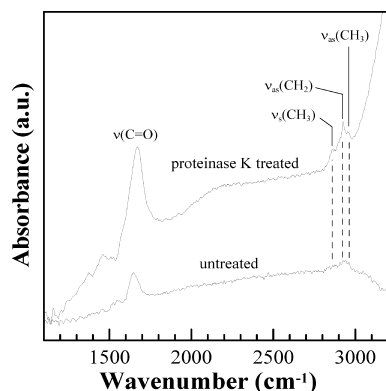


Figure 1. FT-IR spectra of the supernatants obtained from *E. coli* O157:H7 cell suspension before and after enzyme treatment. The supernatant for the IR spectra of the untreated cells was obtained by centrifuging the bacterial cells suspended in Trizma buffer including proteinase K. A Trizma buffer solution including proteinase K prepared separately was used as background.

polyelectrolyte layer. Parameter values of ψ_0 , ψ_{DON} , and κ_m that are required in eq 1 can be calculated using the following equations^{40–43}

$$\psi_0 = \frac{kT}{ze} \left(\ln \left[\frac{\rho_{\text{fix}}}{2zen^\infty} + \left\{ \left(\frac{\rho_{\text{fix}}}{2zen^\infty} \right)^2 + 1 \right\}^{1/2} \right] + \frac{2zen^\infty}{\rho_{\text{fix}}} \left[1 - \left\{ \left(\frac{\rho_{\text{fix}}}{2zen^\infty} \right)^2 + 1 \right\}^{1/2} \right] \right) \quad (2)$$

$$\psi_{\text{DON}} = \frac{kT}{ze} \left(\ln \left[\frac{\rho_{\text{fix}}}{2zen^\infty} + \left\{ \left(\frac{\rho_{\text{fix}}}{2zen^\infty} \right)^2 + 1 \right\}^{1/2} \right] \right) \quad (3)$$

$$\kappa_m = \kappa \left[1 + \left(\frac{\rho_{\text{fix}}}{2zen^\infty} \right)^2 \right]^{1/4} \quad (4)$$

where k is the Boltzmann constant, T is the absolute temperature, e is the elementary electric charge, and z and n^∞ are the valence and bulk number concentration of the electrolyte, respectively. In this work, soft particle theory has been applied to determine and compare the two parameters (i.e., λ^{-1} and ρ_{fix}) for the untreated and proteinase K treated *E. coli* O157:H7 cells using experimentally measured EPM values as a function of IS.

DLVO Interaction Energy. DLVO theory^{23,24} was applied to calculate the interaction energy between cells and quartz before and after enzyme treatment. The interaction energy was determined by the sum of the retarded van der Waals attractive interaction energy⁶⁷ and the electrical double layer interaction energy⁶⁸ for a sphere–plate system. A value of 6.5×10^{-21} J was taken for the Hamaker constant in this case.²² An outer surface potential calculated from the above soft particle formula was used as a cell surface potential at a given IS condition. A quartz surface potential at a given IS condition was obtained from our previous study.³⁸

Results and Discussion

Confirmation of Effectiveness of Enzyme Treatment. The removal of extracellular macromolecules from *E. coli* O157:H7 cell surfaces by proteinase K was confirmed by using FT-IR spectroscopy. Figure 1 shows the IR spectra of supernatants obtained from cell suspension before and after enzyme treatment. Vibrational mode assignments are listed in Table S1 and are consistent with reported values of another *E. coli* O157:H7 strain.⁶⁴ A noticeable difference was observed between the untreated and proteinase K treated cells at the C–H stretching

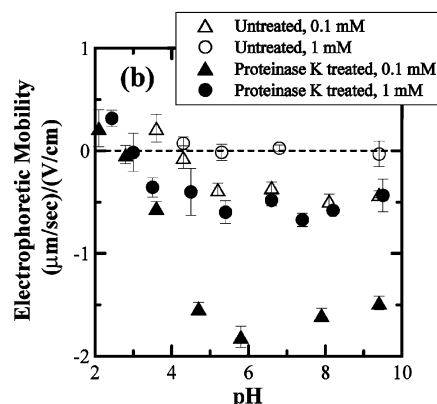
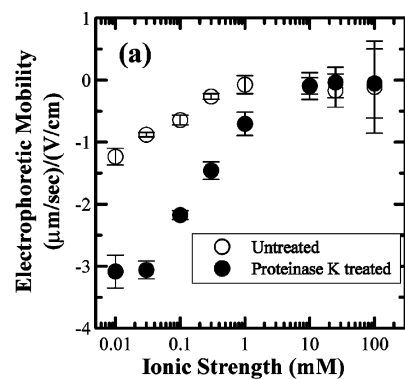


Figure 2. Electrophoretic mobility of untreated and proteinase K treated *E. coli* O157:H7 as a function of (a) IS and (b) pH. In (a), all experiments were performed at unadjusted pH (5.6–5.8). The data for untreated cells conducted at 1, 10, and 100 mM were obtained from ref 38. All experiments were carried out at 25 °C. Error bars indicate one standard deviation.

between 2800–3000 cm^{-1} and C=O stretching at 1653 cm^{-1} . Specifically, an increase of C=O stretching ($\nu(\text{C=O})$) from proteins (at 1653 cm^{-1}), and CH_2 symmetric ($\nu_s(\text{CH}_2)$), CH_3 symmetric ($\nu_s(\text{CH}_3)$), CH_2 asymmetric ($\nu_{\text{as}}(\text{CH}_2)$), and CH_3 asymmetric ($\nu_{\text{as}}(\text{CH}_3)$) stretch from fatty acids (at 2855, 2876, 2926, and 2961 cm^{-1} , respectively)^{64,69} was observed from the supernatant spectra after enzyme treatment. Consistent with the functionality of proteinase K, the results suggest that the peptide bond of the proteins adjacent to C-terminal associated with aliphatic groups and fatty acid structures, which have long carbon chains containing a relatively large number of CH_2 per molecule,^{64,69} were likely removed from the cells by the enzyme reaction. On the other hand, the bands were also observed from the untreated sample with relatively minor peak, which were likely originated from the very low-level removal of extracellular materials after centrifugation.

Influence of Extracellular Macromolecules on Surface Properties of *E. coli* O157:H7. (a) *EPM.* Figure 2a presents the EPM of proteinase K treated and untreated *E. coli* O157:H7 as a function of IS from 0.01 to 100 mM. Over the IS range of 10–100 mM, the EPM values of treated and untreated cells were almost identical (slightly negative) and both were insensitive to changes in IS. Additionally, it was seen that the *E. coli* O157:H7 strain used in this study was almost neutral at IS above 1 mM (Figure 2a) and also insensitive to pH changes over the range of 5.8–9.2 when the IS was between 1 to 100 mM.³⁸ These results suggest that the investigated *E. coli* O157:H7 strain possesses a high buffering capacity under acidic conditions. An insensitivity of EPM with IS and almost neutral EPM under similar conditions have also been reported for other pathogens

(e.g., *E. coli* O157:H7,^{59,70–72} *Salmonella pullorum*,³² *Cryptosporidium parvum* oocysts⁷³). It is interesting to note that the EPM of *E. coli* O157:H7 cells used in this study was relatively low (i.e., less negative) as compared to other nonpathogenic *E. coli* strains.^{74,75}

Over the IS range of 0.01 to 1 mM the magnitude of the EPM value for the untreated *E. coli* O157:H7 gradually decreased with IS (Figure 2a). The proteinase K treated cells followed a similar trend over the IS range of 0.01 to 10 mM. However, the proteinase K enzyme treatment resulted in a higher sensitivity of cell EPM to varying IS than the untreated cells. The observed deviation in the EPM between the treated and untreated cells occurred below 1 mM IS ($P < 0.001$), with the treated cells exhibiting a more negative EPM than their untreated counterparts. A similar trend was observed in a previous study, in which the EPM of *Cryptosporidium parvum* oocysts became more negative after proteinase K treatment.³⁴

To further investigate the influence of enzyme treatment on the nature of charge at the cell surface, EPM of untreated and enzyme treated cells was measured at an IS of 0.1 and 1 mM as a function of pH, which is shown in Figure 2b. The EPM of treated cells became more negative at both 0.1 and 1 mM IS, compared to untreated cells. The IEP of untreated and treated cells were approximately 4.2 and 3.0, respectively, and interestingly the proteinase K treatment results in a shift in the IEP toward slightly lower pH values. The EPM results suggest that the removal of extracellular macromolecules via proteinase K treatment may alter the distribution of functional groups on/ outside the cell surface.

(b) *Potentiometric Titration.* To examine the variation in the distribution of cell surface functional groups before and after proteinase K treatment, pK_a and the corresponding C_i were determined from the potentiometric titration data. Titration results are summarized in Table 2 and Figure 3. As shown in Table 2, the average pK_a values for the untreated cells were determined to be at pH 3.25, 5.14, 7.12, and 8.70 and are likely to be associated with carboxylic/phosphoric/phosphodiester groups, carboxylic group, phosphoric group, and amine or hydroxyl groups, respectively.^{59,61,76} The total site concentration (C_{TOT}) was determined to be 27.4 mol/10¹⁷ cells. The corresponding values of C_i/C_{TOT} were 0.427, 0.179, 0.184, and 0.210 for pK_a values of 3.25, 5.14, 7.12, and 8.70, respectively, suggesting that the carboxylic/phosphoric/phosphodiester groups are likely the dominant functional forms on the *E. coli* O157:H7 cell surface. Castro and Tufenkji⁵⁹ also analyzed the acid–base property of a toxigenic *E. coli* O157:H7 strain and reported that the pK_a values were 3.99, 5.88, 7.70, and 10.55 and the corresponding values of C_i/C_{TOT} were 0.207, 0.138, 0.140, and 0.514, respectively. In contrast to the bacteria used in this study, the *E. coli* strain used by Castro and Tufenkji⁵⁹ apparently possesses a different distribution of charged functional groups on the surface and outside of the cells that are mainly associated with amine or hydroxyl groups (51.4%). Such deviations may occur as a result of differences in nutrient media, growth phase, as well as strains.^{47,61}

Values of pK_a , C_{TOT} , and C_i/C_{TOT} for the proteinase K treated *E. coli* O157:H7 cells are presented in Table 2. The average pK_a values were determined to be 3.27, 4.89, 6.56, and 8.68, and their corresponding C_i/C_{TOT} values were 0.542, 0.188, 0.146, and 0.174, respectively. The pK_a values are consistent for untreated and proteinase K treated cells with no significant difference ($P > 0.05$). Furthermore, the C_1 associated with pK_1 (carboxylic/phosphoric/phosphodiester functional groups) were dominant on both untreated and enzyme treated cells. In contrast,

Table 2. Dissociation Constants (pK_a), Fraction of Site Concentrations (C_i/C_{TOT}), and Total Site Concentrations (C_{TOT}) for Untreated and Proteinase K Treated *E. coli* O157:H7^a

	dissociation constant				fraction of site concentrations ^b			total site concentration (10 ⁻¹⁷ mol/cell)	
	pK_1	pK_2	pK_3	pK_4	C_1/C_{TOT}	C_2/C_{TOT}	C_3/C_{TOT}	C_4/C_{TOT}	C_{TOT}
untreated <i>E. coli</i> O157:H7	3.25 ± 0.06	5.14 ± 0.10	7.12 ± 0.17	8.70 ± 0.08	0.427 ± 0.058	0.179 ± 0.011	0.184 ± 0.051	0.210 ± 0.050	27.41 ± 4.33
proteinase K treated <i>E. coli</i> O157:H7	3.27 ± 0.06	4.89 ± 0.23	6.56 ± 0.40	8.68 ± 0.43	0.542 ± 0.036	0.188 ± 0.037	0.146 ± 0.017	0.174 ± 0.016	18.75 ± 1.89

^a No significant difference ($P > 0.05$) in pK_a values was observed between untreated and proteinase K treated cells. ^b Fraction was calculated using C_i values presented in Figure 3. Dissociation constants (pK_a) and proton binding site concentration (C_i) are determined from potentiometric titration results in 0.1 M KCl using FITEQL 4.0.

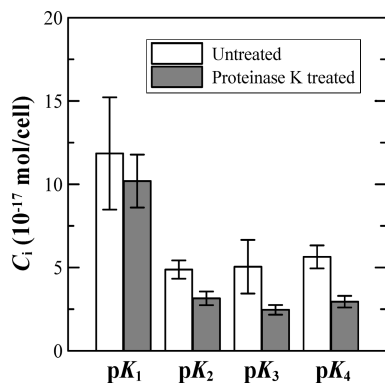


Figure 3. Variation of site concentrations (C_i) at each dissociation constant (pK_a) for untreated and proteinase K treated *E. coli* O157:H7. Error bars indicate one standard deviation.

the value of C_{TOT} for the proteinase K treated cells was up to 22% less than the untreated cells. This result indicates that the proteolytic digestion led to the cleavage and loss of some charged functional groups exposed on the macromolecules in extracellular materials. Figure 3 presents the specific variation in C_i from each pK_a for the untreated and treated cells. A similar amount of functional groups were removed for each C_i ($2 - 2.5 \times 10^{-17}$ mol/cell) after the proteinase K treatment. However, the percent removal was different for each C_i ; with removal of 14.0, 35.5, 51.3, and 47.7% occurring on C_1 , C_2 , C_3 , and C_4 sites, respectively. This observation indicates that the cleavage of functional groups associated with pK_2 , pK_3 , and pK_4 was relatively more pronounced than groups associated with pK_1 .

The relatively small decrease in percent removal of functional groups associated with pK_1 can be explained as follows. As mentioned above, the potential pK_a values associated with certain functional groups are reported as follows:^{61,76,77} carboxylic (2–6; mean 4.5), phosphodiester (3.2–3.5), phosphoric ($pK_{a,1}$: 0.2–2.91 and $pK_{a,2}$: 5.65–7.20), amines (9.1–10.6). Comparison of our data with the reported pK_a values suggest that the removed C_1 , associated with pK_1 , is likely to be due to removal of phosphodiester. Specifically, among these functional groups, phosphoric groups associated with $pK_{a,1}$ would not be captured in this study because they fall outside of the analytical region of the titration (pH range = 0.2–2.91). On the other hand, phosphoric groups associated with $pK_{a,2}$ would be mostly captured in pK_3 . Similarly, carboxylic acid groups are likely to be mostly associated with pK_2 , and they can dissociate over the pH range of 2–6. These observations indicate that the decreased amount of functional groups associated with pK_2 and pK_3 were not necessarily proportional to changes in the functional groups associated with pK_1 .

(c) *Interpretation Using a Soft Particle Theory.* The EPM and titration data for proteinase K treated and untreated *E. coli* O157:H7 clearly showed that the presence of extracellular macromolecules cleaved by proteinase K influenced the electrokinetic and acid–base properties of the cells (Figures 2 and 3, and Table 2). These observations indirectly suggest that the thickness of polymeric layers at the outside of the cells may change with the enzyme treatment.

Soft particle theory^{40–43} was therefore used to further interpret the EPM data as a function of IS and the results are presented in Table 3. The parameters λ^{-1} and ρ_{fix} for the untreated and proteinase K treated *E. coli* O157:H7 were obtained by fitting eq 1 to data shown in Figure 2a using a nonlinear least-squares optimization routine based upon the Levenberg–Marquardt algorithm.⁷⁸ The λ^{-1} values for the untreated and treated cells

Table 3. Calculated Electrophoretic Softness Parameters (λ^{-1}) and Fixed Charge Densities (ρ_{fix}) for Untreated and Proteinase K Treated *E. coli* O157:H7 cells^a

	fixed charge density, ρ_{fix} (mM)	electrophoretic softness, λ^{-1} (nm)
untreated <i>E. coli</i> O157:H7	−0.058	16.31
proteinase K treated <i>E. coli</i> O157:H7	−0.446	7.87

^a The values were obtained by fitting experimentally determined electrophoretic mobility values (0.03–100 mM) using Ohshima's theory (eq 1). Coefficients of linear regression values (r^2) for untreated and proteinase K treated cells are determined to be 0.868 and 0.903, respectively.

were determined to be 16.31 and 7.87 nm, respectively. Here, it should be noted that the λ^{-1} does not mean the length of polymeric layers; instead, the value is related to the extent of the ion-permeable layer.⁴⁵ In addition, the corresponding ρ_{fix} values were found to be −0.058 and −0.446 mM (-5.6×10^3 and -4.3×10^4 C/m³, respectively) for the untreated and treated cells, respectively. The λ^{-1} for the proteinase K treated cells were approximately 50% lower than the untreated cells. The value of ρ_{fix} for the proteinase K treated cells was also quite different than untreated cells, with approximately 8-fold larger magnitude of ρ_{fix} as compared with the untreated cells. Similar trend (i.e., decrease in λ^{-1} and increase in the magnitude of ρ_{fix}) has been reported by Chandraprabha et al. by comparing original *Acidithiobacillus ferrooxidans* cells with LPS-deficient ones.⁷⁹ The differences in λ^{-1} and ρ_{fix} for cells after the enzyme treatment clearly show that the thickness and charged nature of the outside polymeric layer has changed. This implies that considerable length of the extracellular polymeric layer was changed at the outer cell surface. Additionally, the observed trend of an increase in magnitude of ρ_{fix} after the enzyme treatment could be due to the fact that the density of charged ions in deeper parts of the polymeric layers in the vicinity of the cell wall is much greater than that in the outer parts.^{70,80}

Changes in EPM (more negative) and IEP (shifted toward a lower pH) after enzyme treatment are likely related to variations in the distribution of functional groups and the length of macromolecules in the extracellular materials. For soft particles, like bacterial cells, zeta potential determined by EPM represents the surface potential at the slipping plane, whereas the total charge determined by titration accounts for the whole charges from the cell wall surface to the end of polymeric macromolecule layers.^{42,81} The trend that the EPM of the cells became more negative after the enzyme treatment could be due to two reasons. First, results from Ohshima theory calculations (i.e., greater value of ρ_{fix} after enzyme treatment) indicate that cleaved macromolecules in extracellular materials have lower charges per unit volume than remaining macromolecules after enzyme treatment. Second, titration results indicate that the functional groups associated with pK_1 and pK_2 will primarily contribute to the overall net negative charge of the cells at pH 5.8. Hence, observed increases in the relative portion of these acidic sites from approximately 60 to 73% after proteinase K treatment may result in the increased EPM (more negative) and the shift of the IEP from 4.2 to 3.0.

(d) *Hydrophobicity.* Figure 4 presents the percent hydrophobicity of untreated and proteinase K treated *E. coli* O157:H7 cells as a function of IS. The hydrophobicity for the untreated *E. coli* O157:H7 was approximately 26% over the entire range of IS, demonstrating that the cells were consistently hydrophilic. Results observed herein are comparable to previously reported

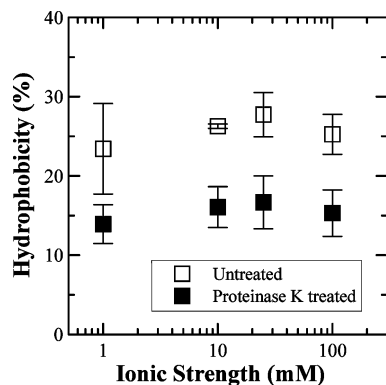


Figure 4. Hydrophobicity of untreated and proteinase K treated *E. coli* O157:H7 as a function of IS. All experiments were performed at unadjusted pH (5.6–5.8). The data for untreated cells conducted at 1, 10, and 100 mM were obtained from ref 38. Error bars indicate one standard deviation.

hydrophobicity values for different *E. coli* O157:H7 strains. Hassan and Frank,⁷⁰ for instance, reported that *E. coli* O157:H7 994 possessed relatively hydrophilic surface property (ca. 4% hydrophobicity as % cells bound to xylene). According to Li and McLandsborough,⁷¹ the hydrophobicity values for six different *E. coli* O157:H7 strains ranged from 25 to 45%, which overlapped with those investigated in this study. Additionally, Castro and Tufenkji⁵⁹ reported that the contact angles of three different *E. coli* O157:H7 strains at two different IS (0.1 and 10 mM KCl) at pH 5.7 were approximately 20° (i.e., hydrophilic) regardless of the changes in strains and IS. It is interesting to note that the *E. coli* O157:H7 exhibited hydrophilic surface characteristics over the range of investigated IS, even while expressing nearly neutral EPM values (Figure 2a).

As shown in Figure 4, the proteinase K treated cells are more hydrophilic than the untreated cells (15% compared with 26%). This trend is consistent with findings from a previous study that reported the hydrophobicity of *Cryptosporidium parvum* oocysts decreased from 39 to 21% at 10 mM KCl (pH 5.8) after proteinase K treatment, which was attributed to the removal of glycosylated proteins covalently bounded to carbohydrates on the oocyst surface.³⁴ Based on the specificity of proteinase K⁵⁵ and the IR spectra data (Figure 1), the major parts of the molecular composition cleaved by proteinase K are likely to be uncharged hydrocarbon-like compounds (C-(C,H)), which are associated with protein/fatty acid structure. It has been reported that the (C-(C,H)) constituents could contribute to the increase in cell hydrophobicity.⁸² Therefore, the decrease in cell hydrophobicity after enzyme treatment is likely due to the removal of (C-(C,H)) constituents mainly from the extracellular polymeric materials.

Influence of Extracellular Macromolecules on Cell Adhesion to Quartz Sand. Figure 5 shows the adhesion efficiency of untreated and proteinase K treated *E. coli* O157:H7 cells on quartz sand as a function of IS. An interesting trend was observed for the untreated cells. Specifically, cell adhesion increased with IS up to 1 mM and then decreased with IS above that point. DLVO interaction energy prediction reveals that the interaction is chemically unfavorable at IS of 0.01 and 0.1 mM (i.e., height of energy barrier = 513 and 10 kT at 0.01 and 0.1 mM, respectively) and chemically favorable at IS \geq 1 mM (i.e., no energy barrier). Hence, the adhesion efficiency for the untreated cells is expected to increase with IS and then reach plateau under chemically favorable conditions. However, the results showed a reverse trend at higher IS (i.e., IS \geq 10 mM). This unanticipated result may

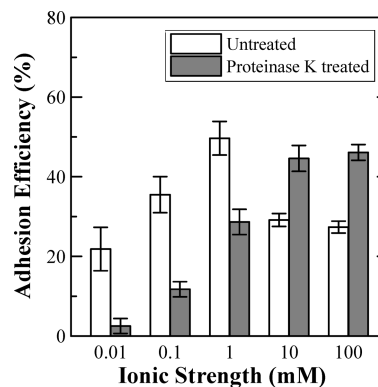


Figure 5. Adhesion efficiency of untreated and proteinase K treated *E. coli* O157:H7 to quartz sand as a function of IS. All experiments were performed at unadjusted pH (5.6–5.8). Error bars indicate one standard deviation.

be attributed to electrosteric repulsion at high IS due to the conformational change (i.e., more brushlike) of polymeric layers outside the cell surface.^{19,34,37,71} Additional support for this hypothesis is obtained by comparing with the adhesion behavior of proteinase K treated cells (Figure 5). Specifically, the adhesion efficiency for proteinase K treated cells increased with IS up to 10 mM and then reached a plateau (i.e., adhesion efficiency of 3, 12, 29, 45, and 46% at IS of 0.01, 0.1, 1, 10, and 100 mM, respectively). In contrast to the untreated cells, this trend was consistent with DLVO interaction energy predictions in that there is an energy barrier of 2423, 339, and 5 kT when the IS was 0.01, 0.1, and 1 mM, respectively, but no energy barrier when the IS was 10 and 100 mM. Comparison of the adhesion efficiency between the untreated and the proteinase K treated cells clearly demonstrates that the abnormal trend with IS under favorable conditions for the untreated cells is likely due to the electrosteric repulsion due to the presence of extracellular macromolecules. It should also be mentioned that the treated cells exhibited less adhesion than the untreated cells when the IS \leq 1 mM due to their more negative electrophoretic mobility (Figure 2a).

Concluding Remarks. In conclusion, experimental and modeling work has been conducted to investigate the role of extracellular macromolecules on phenotypic properties and adhesion behavior of enterohemorrhagic *E. coli* O157:H7. Thorough surface characterization of untreated and proteinase K treated cells indicated that partial removal of extracellular macromolecules led to changes in the cell surface properties. Specifically, enzyme treatment led to a decrease in the overall charge density (titration), to less electrophoretically soft outermost layers of the cells, and to more negative and hydrophilic macroscopic surface properties. Although the change in cell surface properties after enzyme treatment seemed to be small in the magnitude, they produced very significant differences in the cell adhesion tests. Under favorable conditions (IS > 1 mM), a sudden decrease in the removal efficiency was observed for untreated cells. In contrast, adhesion of treated cells increased and then reached the plateau with IS in a manner that was consistent with predictions of the DLVO theory. These results suggested that another non-DLVO type interaction (i.e., electrosteric repulsion) occurred with the untreated cells when the IS > 1 mM due to the presence of extracellular macromolecules. Findings from this study provide insight on the limitations of traditional approaches to predict adhesion of *E. coli* O157:H7 cells. Furthermore, this study suggests that a combined

approach, molecular-level as well as macroscopic-level analyses, is necessary to better understand the potential role of macromolecule-induced interactions on *E. coli* O157:H7 fate in aquatic environments.

Acknowledgment. This research was funded by the USDA CSREES NRI (Grant No. 2006-02541). The *E. coli* O157:H7/pGFP strain 72 was provided by Dr. Pina Fratamico (USDA-ARS-ERRC, Wyndmoor, PA). We acknowledge Dr. Francisco Zaera (Department of Chemistry, University of California, Riverside) for his FT-IR expertise and access to his equipment.

Supporting Information Available. Potentiometric titration curves for blank and bacterial solutions (Figure S1) and vibrational mode assignments for the FT-IR spectra of *E. coli* O157:H7 in Figure 1 (Table S1). This material is available free of charge via the Internet at <http://pubs.acs.org>.

References and Notes

- Riley, L. W.; Remis, R. S.; Helgerson, S. D.; McGee, H. B.; Wells, J. G.; Davis, B. R.; Hebert, R. J.; Olcott, E. S.; Johnson, L. M.; Hargrett, N. T.; Blake, P. A.; Cohen, M. L. *N. Engl. J. Med.* **1983**, *308*, 681–685.
- Tremoulet, F.; Duche, O.; Namane, A.; Martinie, B.; Labadie, J.-C. *FEMS Microbiol. Lett.* **2002**, *215*, 7–14.
- Kaper, J. B.; Karmali, M. A. *Proc. Natl. Acad. Sci.* **2008**, *105*, 4535–4536.
- Nwachuku, N.; Gerba, C. P., *Rev. Environ. Sci. Biotechnol.* **2008**, DOI 10.1007/s11157-008-9132-0.
- Kaper, J. B.; Nataro, J. P.; Mobley, H. L. T. *Nature Rev.* **2004**, *2*, 123–140.
- Potter, A. A.; Klashinsky, S.; Li, Y.; Frey, E.; Townsend, H.; Rogan, D.; Erickson, G.; Hinkley, S.; Klopfenstein, T.; Moxley, R. A.; Smith, D. R.; Finlay, B. B. *Vaccine* **2004**, *22*, 362–369.
- Centers for Disease Control and Prevention; *Morb. Mortal. Wkly. Rep.* **2006**, *55*, pp 1045–1046;
- Islam, M.; Doyle, M. P.; Phatak, S. C.; Millner, P.; Jiang, X. *J. Food Prot.* **2004**, *67*, 1365–1370.
- Rangel, J. M.; Sparling, P. H.; Crowe, C.; Griffin, P. M.; Swerdlow, D. L. *Emerg. Infect. Dis.* **2005**, *11*, 603–609.
- Armstrong, G. L.; Hollingsworth, J.; Morris, J. G., Jr. *Epidemiol. Rev.* **1996**, *18*, 29–51.
- Olsen, S. J.; Miller, G.; Breuer, T.; Kennedy, M.; Higgins, C.; Walford, J.; McKee, G.; Fox, K.; Bibb, W.; Mead, P. *Emerg. Infect. Dis.* **2002**, *8*, 370–375.
- Hunter, P. J. *Water Health* **2003**, *1*, 65–72.
- Curriero, F. C.; Patz, J. A.; Rose, J. B.; Lele, S. *Am. J. Public Health* **2001**, *91*, 1194–1199.
- Thomas, K. M.; Charron, D. F.; Waltner-Toews, D.; Schuster, C.; Maarouf, H.; J. D. *Int. J. Environ. Health Res.* **2006**, *16*, 167–180.
- Law, D. J. *Appl. Microbiol.* **2000**, *88*, 729–745.
- Ryu, J.-H.; Beuchat, L. R. *Appl. Environ. Microbiol.* **2005**, *71*, 247–254.
- Seltmann, G.; Holst, O. *The Bacterial Cell Wall*; Springer: Berlin, New York, 2002.
- McSwain, B. S.; Irvine, R. L.; Hausner, M.; Wilderer, P. A. *Appl. Environ. Microbiol.* **2005**, *71*, 1051–1057.
- Chen, G.; Walker, S. L. *Langmuir* **2007**, *23*, 7162–7169.
- Poortinga, A. T.; Bos, R.; Norde, W.; Busscher, H. J. *Surf. Sci. Rep.* **2002**, *47*, 1–32.
- Poortinga, A. T.; Bos, R.; Busscher, H. J. *Colloids Surf., B* **2001**, *20*, 105–117.
- Redman, J. A.; Walker, S. L.; Elimelech, M. *Environ. Sci. Technol.* **2004**, *38*, 1777–1785.
- Derjaguin, B. V.; Landau, L. D. *Acta Physicochim. U.S.S.R* **1941**, *14*, 300.
- Verwey, E. J. W.; Overbeek, J. T. G. *Theory of the stability of lyophobic colloids: the interaction of sol particles having an electric double layer*; Elsevier: Amsterdam, 1948.
- Azaredo, J.; Visser, J.; Oliveira, R. *Colloids Surf., B* **1999**, *14*, 141.
- Ong, Y. L.; Razatos, A.; Georgiou, G.; Sharma, M. M. *Langmuir* **1999**, *15*, 2719–2725.
- O'Brien, R. W.; White, L. R. *J. Chem. Soc., Faraday Trans.* **1978**, *74*, 1607–1626.
- von Smoluchowski, M. *Phys. Chem. (Muenchen, Ger.)* **1918**, *92*, 129.
- Hayashi, H.; Tsuneda, S.; Hirata, A.; Sasaki, H. *Colloids Surf., B* **2001**, *22*, 149–157.
- Morisaki, H.; Nagai, S.; Ohshima, H.; Ikemoto, E.; Kogure, K. *Microbiology* **1999**, *145*, 2797–2802.
- Kiers, P. J. M.; Bos, R.; van der Mei, H. C.; Busscher, H. J. *Microbiology* **2001**, *147*, 757–762.
- Haznedaroglu, B. Z.; Kim, H. N.; Bradford, S. A.; Walker, S. L. *Environ. Sci. Technol.* **2009**, *43*, 1838–1844.
- Israelachvili, J. N. *Intermolecular and surface forces*, 2nd ed.; Academic Press: Amsterdam, Boston, 1992.
- Kuznar, Z. A.; Elimelech, M. *Environ. Sci. Technol.* **2006**, *40*, 1837–1842.
- Walker, S. L.; Redman, J. A.; Elimelech, M. *Langmuir* **2004**, *20*, 7736–7746.
- Burks, G. A.; Velegol, S. B.; Paramonava, E.; Lindenmuth, B. E.; Feick, J. D.; Logan, B. E. *Langmuir* **2003**, *19*, 2366–2371.
- Kuznar, Z. A.; Elimelech, M. *Langmuir* **2005**, *21*, 710–716.
- Kim, H. N.; Bradford, S. A.; Walker, S. L. *Environ. Sci. Technol.* **2009**, *43*, 4340–4347.
- Liu, Y.; Yang, C.-H.; Li, J. *Environ. Sci. Technol.* **2007**, *41*, 198–205.
- Ohshima, H. *J. Colloid Interface Sci.* **1994**, *163*, 474–483.
- Ohshima, H.; Kondo, T. *J. Colloid Interface Sci.* **1989**, *130*, 281–282.
- Ohshima, H. *Colloids Surf., A* **1995**, *103*, 249–255.
- Ohshima, H.; Kondo, T. *Biophys. Chem.* **1991**, *39*, 191–198.
- Bos, R.; van der Mei, H. C.; Busscher, H. J. *Biophys. Chem.* **1998**, *74*, 251–255.
- Rodriguez, V. V.; Busscher, H. J.; Norde, W.; van der Mei, H. C. *Electrophoresis* **2002**, *23*, 2007–2011.
- Takashima, S.; Morisaki, H. *Colloids Surf., B* **1997**, *9*, 205–212.
- Eboigbodun, K. E.; Ojeda, J. J.; Biggs, C. A. *Langmuir* **2007**, *23*, 6691–6697.
- Ojeda, J. J.; Romero-Gonzalez, M. E.; Bachmann, R. T.; Edyvean, R. G. J.; Banwart, S. A. *Langmuir* **2008**, *24*, 4032–4040.
- Tourney, J.; Ngwenya, B. T.; Fred Mosselmans, J. W.; Tetley, L.; Cowie, G. L. *Chem. Geol.* **2008**, *247*, 1–15.
- van der Mei, H. C.; Weerkamp, A. H.; Busscher, H. J. *FEMS Microbiol. Lett.* **1987**, *40*, 15–19.
- Walker, S. L.; Hill, J. E.; Redman, J. A.; Elimelech, M. *Appl. Environ. Microbiol.* **2005**, *71*, 3093–3099.
- Bradford, S. A.; Simunek, J.; Walker, S. L. *Water Resour. Res.* **2006**, *42*, W12S12, DOI: 10.1029/2005WR004805.
- Yao, K. M.; Habibian, M. T.; O'Melia, C. R. *Environ. Sci. Technol.* **1971**, *5*, 1105–1112.
- Fratamico, P. M.; Deng, M. Y.; Strobaugh, T. P.; Palumbo, S. A. *J. Food Prot.* **1997**, *60*, 1167–1173.
- Ebeling, W.; Hennrich, N.; Klockow, M.; Metz, H.; Orth, H. D.; Lang, H. *Eur. J. Biochem.* **1974**, *47*, 91–97.
- Boulos, L.; Prevost, M.; Barbeau, B.; Coallier, J.; Desjardins, R. *J. Microbiol. Methods* **1999**, *37*, 77–86.
- American Public Health Association, American Water Works Association, Water Pollution Control Federation. *Standard Methods for the Examination of Water and Wastewater*, 20th ed.; American Public Health Association: Washington DC, 1998.
- Pembrey, R. S.; Marshall, K. C.; Schneider, R. P. *Appl. Environ. Microbiol.* **1999**, *65*, 2877–2894.
- Castro, F. D.; Tufenkji, N. *Environ. Sci. Technol.* **2007**, *41*, 4332–4338.
- Herbelin, A. L.; Westall, J. C. FITEQL: A Computer Program for Determination of Chemical Equilibrium Constants from Experimental Data. Report 99-01; Department of Chemistry, Oregon State University: Corvallis, OR, 1999.
- Hong, Y.; Brown, D. G. *Colloids Surf., B* **2006**, *50*, 112–119.
- Daughney, C. J.; Fein, J. B.; Yee, N. *Chem. Geol.* **1998**, *144*, 161.
- Kansiz, M.; Heraud, P.; Wood, B.; Burden, F.; Beardall, J.; McNaughton, D. *Phytochemistry* **1999**, *52*, 407–417.
- Al-Qadiri, H. M.; Lin, M.; Cavinato, A. G.; Rasco, B. A. *Int. J. Food Microbiol.* **2006**, *111*, 73–80.
- Mirabella, F. M. *Internal reflection spectroscopy: Theory and applications*; Mirabella, F. M., Ed.; Marcel Dekker: New York, 1993.
- Tufenkji, N.; Miller, G. F.; Ryan, J. N.; Harvey, R. W.; Elimelech, M. *Environ. Sci. Technol.* **2004**, *38*, 5932–5938.
- Gregory, J. J. *Colloid Interface Sci.* **1981**, *83* (1), 138–145.
- Hogg, R. I.; Healey, T. W.; Fuerstenau, D. W. *Trans. Faraday Soc.* **1966**, *62*, 1638–1651.

- (69) Schmitt, J.; Flemming, H.-C. *Int. Biodeterior. Biodegrad.* **1998**, *41*, 1–11.
- (70) Hassan, A. N.; Frank, J. F. *Int. J. Food Microbiol.* **2004**, *96*, 103–109.
- (71) Li, J.; McLandsborough, L. A. *Int. J. Food Microbiol.* **1999**, *53*, 185–193.
- (72) Lytle, D. A.; Rice, E. W.; Johnson, C. H.; Fox, K. R. *Appl. Environ. Microbiol.* **1999**, *65*, 3222–3225.
- (73) Tufenkji, N.; Elimelech, M. *Environ. Sci. Technol.* **2005**, *39*, 3620–3629.
- (74) Kim, H. N.; Walker, S. L. *Colloids Surf., B* **2009**, *71*, 160–167.
- (75) Bolster, C. H.; Haznedaroglu, B. Z.; Walker, S. L. *J. Environ. Qual.* **2009**, *38*, 465–472.
- (76) Martinez, R. E.; Smith, D. S.; Kulczycki, E.; Ferris, F. G. *J. Colloid Interface Sci.* **2002**, *253*, 130–139.
- (77) Cox, J. S.; Smith, S.; Warren, L. A.; Ferris, F. G. *Environ. Sci. Technol.* **1999**, *33*, 4514–4521.
- (78) Marquardt, D. W. *SIAM J. Appl. Math.* **1963**, *11*, 431–441.
- (79) Chandraprabha, M. N.; Modak, J. M.; Natarajan, K. A. *Colloids Surf., B* **2009**, *69*, 1–7.
- (80) van Loosdrecht, M. C. M.; Lyklema, J.; Norde, W.; Schraa, G.; Zehnder, A. J. B. *Appl. Environ. Microbiol.* **1987**, *53*, 1898–1901.
- (81) Hong, Y.; Brown, D. G. *Langmuir* **2008**, *24*, 5003–5009.
- (82) Hamadi, F.; Latrache, H.; Zahir, H.; Elghmari, A.; Timinouni, M.; Ellouali, M. *Braz. J. Microbiol.* **2008**, *39*, 10–15.

BM900516Y